

# Fractional Magnetization Plateaus and Magnetic Order in the Shastry Sutherland Magnet $\text{TmB}_4$

K. Siemensmeyer,<sup>1</sup> E. Wulf,<sup>1</sup> H.-J. Mikeska,<sup>2</sup> K. Flachbart,<sup>3</sup> S. Gabáni,<sup>3</sup>  
S. Maťaš,<sup>3</sup> P. Priputen,<sup>3</sup> A. Efdokimova,<sup>4</sup> and N. Shitsevalova<sup>4</sup>

<sup>1</sup>*Hahn Meitner Institut Berlin, Glienicker Str. 100, D 14109 Berlin, Germany*

<sup>2</sup>*Institut für Theoretische Physik, Universität Hannover, 30167 Hannover, Germany*

<sup>3</sup>*Institute of Experimental Physics, Slovak Academy of Science, SK 04001 Kosice, Slovakia*

<sup>4</sup>*Institute for Problems of Material Science, Ukraine Academy of Science, UA 03680 Kiev, Ukraine*

(Dated: October 25, 2018)

We investigate the phase diagram of  $\text{TmB}_4$ , an Ising magnet on a frustrated Shastry-Sutherland lattice by neutron diffraction and magnetization experiments. At low temperature we find Néel order at low field, ferrimagnetic order at high field and an intermediate phase with magnetization plateaus at fractional values  $M/M_{\text{sat}} = 1/7, 1/8, 1/9 \dots$  and spatial stripe structures. Using an effective  $S = 1/2$  model and its equivalent two-dimensional (2D) fermion gas we suggest that the magnetic properties of  $\text{TmB}_4$  are related to the fractional quantum Hall effect of a 2D electron gas.

PACS numbers: 73.43.Nq, 71.10Pm, 71.20.Eh, 75.25+z

The magnetic properties of quantum spins with antiferromagnetic (afm) coupling on frustrating lattices have attracted widespread interest in recent years due to the discovery of new types of complex quantum ground states. Recent examples include the spin liquid dimer phase observed in  $\text{SrCu}_2(\text{BO}_3)_2$  [1] (a 2D magnet on the Shastry-Sutherland lattice (SSL) [2]), supersolid phases on triangular and kagome lattices [3] and the spin ice state in pyrochlore [4]. The interest in such systems is in particular in magnetization plateaus at fractional values of the saturation magnetization as observed in  $\text{SrCu}_2(\text{BO}_3)_2$  [5] and in fractionalized excitations as discussed for spin ice [6], in particular the possible existence of a magnetic monopole [7]. This documents that plateaus and fractional excitations which are well known in quantum Hall physics also emerge in quantum magnets.

A relation between magnetization plateaus in 2D quantum spin systems and the quantum Hall effect was established by a mapping of 2D  $S=1/2$  magnets to the 2D electron gas [8], requiring an additional Chern-Simons field, a fictitious nonlocal strong magnetic field. When this field is spatially averaged it combines with lattice induced minigaps (known from the 'Hofstadter butterfly' [9]) to induce fractional magnetization plateaus. In simulations using this approach fractional magnetization plateaus down to values as small as  $M_{\text{sat}} = 1/9$  have recently been reported [10] together with complex modulated spatial structures of the corresponding ground states. For investigations of these phenomena in  $\text{SrCu}_2(\text{BO}_3)_2$ , however, the very high critical field in this material is a severe limit and complex spatial structures have not been found experimentally so far.

In the following we present the results of magnetization and neutron diffraction experiments for  $\text{TmB}_4$ , another 2D magnet on a SSL and fully accessible to experiments up to the saturation field. We suggest that this compound is an excellent realization of a frustrated mag-

net on the SSL, we find the emergence of fractionalized magnetization plateaus strikingly similar to the case of  $\text{SrCu}_2(\text{BO}_3)_2$  and we observe spatial structures similar to those described in Ref. 10. We find it attractive to speculate, on the basis of experimental results to be described in the following, that  $\text{TmB}_4$  represents a magnetic analogue to the fractional quantum Hall effect (FQHE).

$\text{TmB}_4$  belongs to a group of rare earth tetraborides ( $\text{REB}_4$ ) that crystallize in a tetragonal lattice (space group 127) [11]. The rare earth moment position can be mapped to a SSL with nearly equivalent bond lengths between nearest neighbors. In contrast to  $\text{SrCu}_2(\text{BO}_3)_2$ , however, (i)  $\text{TmB}_4$  is a metal and (ii) the  $\text{Tm}^{3+}$  moment is  $J = 6$  and subject to strong crystal field (CF) effects. Thus the RKKY interaction is expected to be important and the basic spin model is an effective  $S=1/2$  model close to the Ising limit rather than a Heisenberg model.

*Experimental:* Single crystals of  $\text{TmB}_4$  were grown by an inductive, crucible-free zone melting method. The residual resistivity ratio was larger than 100, documenting the high sample quality. The neutron sample had cylindrical shape with a diameter of  $\approx 7\text{mm}$  and a length of  $\approx 20\text{mm}$ , isotope enriched  $^{11}\text{B}$  was used to reduce the absorption. For magnetization experiments oriented samples were cut with approximate dimension  $1\times 1\times 1\text{mm}^3$ . Magnetization data were measured using a commercial magnetometer [12]. For neutron diffraction experiments we have used the E10 diffractometer at the HMI [13]. A wavelength of  $0.14\text{nm}$  was obtained from a Ge (220) monochromator. The  $\lambda/2$  contamination was removed by Sapphire- and PG-filters.

*Macroscopic properties:*  $\text{TmB}_4$  shows a rich phase diagram as a function of field and temperature (Fig. 1(a)) [14, 15]. In zero field magnetic order sets in at  $T_N = 11.8\text{K}$ , the afm low temperature Néel phase is stable below  $9.8\text{K}$ . Based on magnetization experiments, at low temperature three phases are seen: The 'high' field

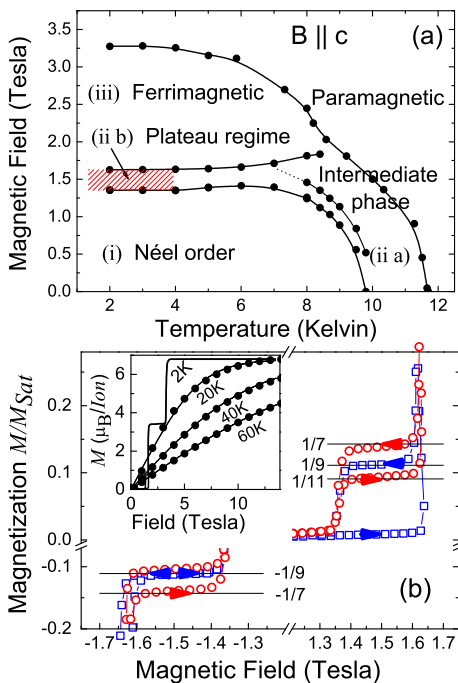


FIG. 1: (a) The phase diagram of  $\text{TmB}_4$  as derived from magnetization data for  $B \parallel (001)$  (full symbols). (b) Magnetization at  $T = 2\text{K}$  (open squares) and  $T = 3\text{K}$  (open circles). The arrows indicate the direction of the field change. The inset in (b) gives an overview towards high field, lines are measured data, full circles are calculated using the high temperature approximation. The magnetic field data are corrected for demagnetization.

phase is ferrimagnetic with a plateau at  $M/M_{\text{sat}} = 1/2$ . In the intermediate phase, magnetization plateaus with  $M/M_{\text{sat}} = 1/7, 1/8, 1/9 \dots$  are seen at temperatures below  $4\text{K}$ . Their observation is subject to hysteresis. After zero field cooling plateaus are observed only when the ferrimagnetic phase has been reached once, but then independent on the direction of the magnetic field changes and the field direction. The value of plateau magnetization varies between different runs: although the energy difference between plateaus may be very small, the time required for a significant spatial rearrangement of moments likely exceeds the time available experimentally. We note that close to  $T_N$  the intermediate phase splits into more complex phases as identified in specific heat and resistivity measurements [15, 16], but with little signature in neutron diffraction and magnetization experiments.

The single ion magnetic ground state is derived from the magnetic specific heat [16] combined with magnetization data: The specific heat can be analyzed in terms of a CF Hamiltonian  $H = -g\mu_B B S_z + D S_z^2$  where  $D < 0$  is the CF anisotropy. Towards high temperature, the entropy reaches the value  $R \ln 2$  which suggests an effective doublet ground state for the noninteracting  $\text{Tm}^{3+}$  ion.

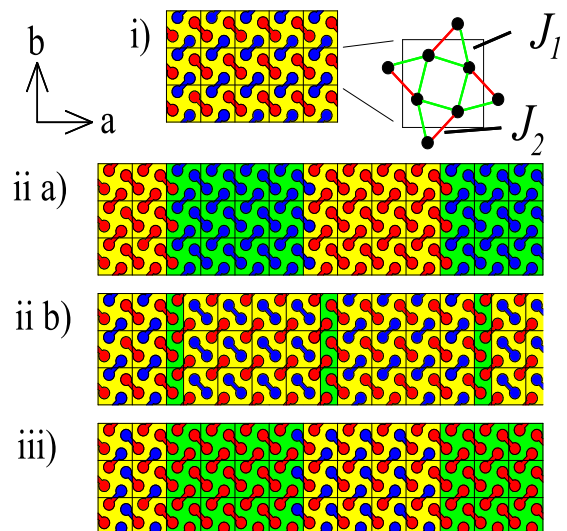


FIG. 2: The magnetic structure of Ising spins in  $\text{TmB}_4$  in the tetragonal plane. Only domains along the  $a$ -direction are shown. Red(blue) circles indicate up(down) moments, the different colors indicate the periodicity of the various stripe structures. Labels (i) to (iii) refer to the phase labels as used in Fig. 1(a). In (i) the position of the  $\text{Tm}^{3+}$  ions in the tetragonal plane is expanded with the SS bonds marked in red. Note the almost identical length of exchange paths  $J_1$  and  $J_2$ .

At low temperature, for magnetic field parallel to the  $c$ -axis, the magnetization reaches the saturation moment of  $\text{Tm}^{3+}$  for  $B > 5\text{T}$ . Therefore, the local single ion ground state is the doublet  $M_J = \pm 6$ , implying that the degeneracy of the  $J = 6$  multiplet is completely lifted by the CF. The splitting between ground state and first excited state can be estimated from the Schottky anomaly [16], yielding  $D = 11\text{K}$ . Consequently, the first excited doublet with  $M_J = \pm 5$  is at  $\approx 100\text{K}$  and strong Ising anisotropy is expected. However, transverse exchange will have to be added to the dominant Ising coupling to improve the agreement of magnetization and specific heat data to results for an ideal Ising model.

*Magnetic structure:* The low temperature - zero field structure is the Néel antiferromagnet (Fig. 2(i)) with moments along the  $(001)$  direction, implying ferromagnetic (fm) correlations along the Shastry-Sutherland (SS) bonds. This follows from the observation of  $(100)$  and  $(300)$  reflections and the absence of af intensity along  $(00L)$ .

The diffraction data for the high temperature phase (Fig. 2(ii a)) close to  $T_N$  at  $B = 0$  agree well with an amplitude modulated structure of fm stripes parallel to the  $a$ -axis, separated by a  $\pi$  domain wall. Any 'checkerboard' arrangements in diagonal blocks can be excluded.

For neutron investigations of the intermediate phase field cooling was used to avoid the hysteresis. This leads to the coexistence of magnetic structures with

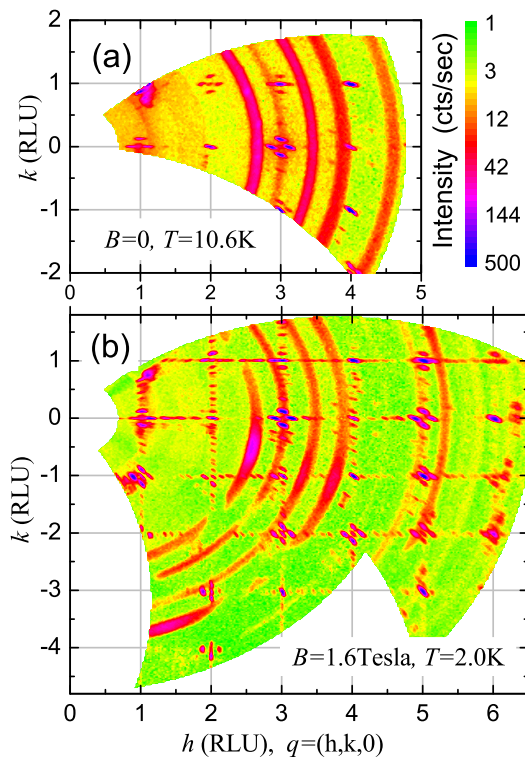


FIG. 3: (a) and (b) show the neutron diffraction pattern in the tetragonal plane for the intermediate and the plateau phase, respectively. The figures share the intensity color code given in (a). For the indexing of the afm peaks see the text. The powder lines arise from aluminum in the ‘Orange’ cryostat (a) and the ‘VM3’ magnet cryostat [13] used for experiments in a field (b).

different unit cell size: Fig. 3(b) shows a diffraction pattern with reflections that may be indexed by  $(2m/7, 0, 0)$ ,  $(2m/9, 0, 0)$ ,  $(n/7, K, 0) \dots$ , where  $m, n$  are integers. Lines of weak “harmonic” reflections result from stripe structures parallel to the  $(H00)$  or  $(0K0)$  direction with a size 7 or 9 unit cells (Fig. 2(ii b)), directly related to the magnitude of the observed magnetization plateaus with  $M/M_{\text{sat}} = 1/7, 1/9$ . In addition, the afm reflections known from the zero field Néel phase have significant intensity, giving evidence for fm correlations along the SS bonds.

The ferrimagnetic high field phase shows again peaks indexed by  $1/8$ , indicating a large unit cell. Using the experimental result  $M/M_{\text{sat}} = 1/2$ , it can be analyzed similarly to the intermediate phase. Here the fm correlations along the SS diagonals are changed to afm for  $1/2$  of the large magnetic unit cell (Fig. 2(iii)) whereas the remaining moments are just fm. This again results in a stripe structure, any diagonal arrangement of the moments can be excluded.

To summarize the experimental results we conclude that the spin interactions appear to be (i) antiferromagnetic, (ii) highly anisotropic and (iii) governed by the

Ising like CF anisotropy. They lead to stripe structures and magnetization plateaus that resemble the predictions for  $\text{SrCu}_2(\text{BO}_3)_2$ .

*Effective  $S = 1/2$  model:* For the interpretation of the experimental data at low temperatures we use an effective  $S = 1/2$  Ising model on the SSL with afm exchange  $J_1 > 0$  on the square bonds and  $J_2 > 0$  on diagonal bonds. In the ideal Ising limit (zero transverse exchange) the ground state of the model is the Néel state for  $J_1 > J_2/2$  and an Ising dimer state (opposite spins on the SS diagonals) for  $J_1 < J_2/2$ . Starting from the Néel ground state, an applied field induces a  $1/2$  magnetization plateau for  $2J_1 - J_2/2 < \mu_B B < 2J_1 + J_2/2$  and saturation at still higher fields with discontinuous transitions between these states. From the data on the extent of the Néel and  $1/2$  plateau phases we conclude  $J_2 \approx J_1$ , in agreement with the exchange paths expected from the geometric structure. An additional transverse exchange (exchanging effective spin components  $+\frac{1}{2}$  and  $-\frac{1}{2}$ ) will broaden the discontinuous transitions in an applied field. Transverse exchange, however, will be small due to the strong single ion anisotropy and numerical calculations of the magnetization for a 16 spin SSL show that the broadening is below the experimentally observable limit for an xy-anisotropy  $\epsilon < 0.1$ .

For an understanding of the rich superstructures and of the fractional plateaus observed in the regime intermediate between afm and ferrimagnetic order, the Ising limit is not sufficient (the spatial period in this regime is just doubled compared to the period of the Néel phase) and in fact several higher order corrections may contribute to the observed features such as additional exchange interactions between further neighbors resulting from RKKY interactions and magnetoelastic effects [18].

Whereas RKKY interaction effects appear as the natural choice to describe complex spatial structures in a rare earth compound and have, in addition to Ising exchange, in fact been used to describe e.g. a variety of spatial structures in the compound  $\text{CeSb}$  [19], this will require very special interaction ratios over large distances. Considering the similarity to  $\text{SrCu}_2(\text{BO}_3)_2$  this nongeneric description is not satisfying and we find it worthwhile to consider as alternative possibility the influence of the transverse exchange using the concepts applied to magnets on the SSL before [8]. These concepts in fact do provide a much more natural approach for an understanding of the experimental findings in  $\text{TmB}_4$ . In the following we thus speculate that  $\text{TmB}_4$  could be considered as equivalent to a 2D spinless fermion gas in a very strong magnetic field. This will lead to a proposal for the understanding of plateaus and the accompanying spatial structures in parallel to the corresponding interpretation of the high field phenomena in the well investigated compound  $\text{SrCu}_2(\text{BO}_3)_2$  [8, 10, 17]. This interpretation is based on (i) the mapping of spins  $1/2$  to hard core bosons and (ii) the subsequent mapping of hard core bosons to

fermions. In 2D, step (ii) requires the introduction of a fictitious magnetic field, the Chern-Simons field  $H_{CS}$  with vector potential  $\mathbf{a}(r)$  and flux  $\Phi(r)$  determined by the fermion density  $\rho(r)$ , given by  $\nabla \times \mathbf{a} = \phi_0 \rho(r) \mathbf{e}_z$  and  $\Phi(r) = 2\pi\rho(r)$ . Here,  $\phi_0$  is the flux quantum and  $\Phi(r)$  is the flux through a plaquette adjacent to lattice point  $r$  (choose once and for all one of the 4 plaquettes adjacent to a point  $r$  with the fermion density  $\rho(r) = S_r^z + \frac{1}{2}$ ). Apart from this fictitious magnetic field  $H_{CS}$  there is an effective fermion hamiltonian with band width determined by the transverse exchange and interaction determined by the Ising part of the magnetic exchange  $J^z$ .

If the nonlocal vector potential attached to each fermion is treated in the average flux approximation as described in Ref.[8], the problem is reduced to a gas of interacting spinless fermions in a strong magnetic field characterized by an average flux related to the magnetization  $M$  of the original magnetic model

$$\Phi = 2\pi\langle\rho(r)\rangle = 2\pi \left( \langle S^z \rangle + \frac{1}{2} \right) = 2\pi \left( M + \frac{1}{2} \right)$$

A noninteracting electron gas on the square lattice has been studied starting from a tight binding band [9] as well as from Landau levels [20, 21, 22, 23], both approaches showing the emergence of a fractal structure due to the periodic lattice potential, the Hofstadter butterfly. Starting from Landau levels leads more directly to the quantum Hall effect: Landau band splits into  $p$  subbands, minigaps result which should be observable in additional plateaus of the Hall conductance. Whereas a direct experimental observation is not possible due to the extremely high magnetic fields required, these minigaps may have been observed experimentally using superlattice structures [24]. In our case the relevant magnetic field is not the physical field but the fictitious field from the Chern-Simons term which produces magnetic flux of the order of a flux quantum per site. It has been shown in Ref.[8] that the conductance plateaus resulting from the combination of discreteness and fictitious Chern-Simons field can be identified as some of the magnetization plateaus observed in  $\text{SrCu}_2(\text{BO}_3)_2$ . This was done by using the SSL instead of the square lattice and treating the electron interaction in mean field approximation. The present case is similar in that the SSL applies also for  $\text{TmB}_4$ , but is different in that the electron interaction is strong due to the dominating Ising term in the magnetic hamiltonian. Thus the situation is that of electrons on a SSL in the regime of the FQHE and the plateaus of interest will result from the combined effect of the lattice (leading to minigaps) and of electron-electron interactions (leading to the gaps of the FQHE), a combination which is expected to result in a large variety of possible plateaus. We therefore speculate that  $\text{TmB}_4$  is a magnetic analogon of the FQHE on a periodic lattice.

Our investigations have shown that the Ising like 2D SS magnet  $\text{TmB}_4$  is characterized by unusual magnetization

plateaus at small fractional values ( $1/7, 1/9 \dots$ ), tied to complex spatial structures. We have speculated that a consistent description of plateaus and spatial structures may be obtained from a mapping of this model to the FQHE in a 2D electron gas with strong Coulomb interactions on a lattice in high field. Whereas alternative interpretations should not be excluded at the moment, our speculation, if true, would open up the new field of studying quantum states similar to the FQHE in magnetic materials. We hope that this work stimulates further investigations although, in view of the efforts to relate microscopic numerical calculations for interacting electrons to the FQHE [25], the numerical work required may be beyond the present possibilities.

*Acknowledgements:* We have the pleasure the acknowledge stimulating discussions with R. Haug, B. Lake, M. Meissner, A. Tennant and K. Totsuka. This work in part was supported by INTAS and DAAD, by Slovak Agencies VEGA (7054) and APVT (0166), and US Steel Kosice.

- 
- [1] H. Kageyama et al, Phys. Rev. Lett. **82**, 3168 (1999).
  - [2] B. S. Shastry and B.Sutherland, Physica **108B**, 1069 (1981).
  - [3] R. Moessner and S. L. Sondhi, Phys. Rev. B **63**, 224401 (2001)
  - [4] S. T. Bramwell and M. J. P. Gingras, Science **294**, 1495 (2001)
  - [5] K. Kodama et al, Science **298**, 395 (2002).
  - [6] P. Fulde, K. Penc and N. Shannon, Ann. Phys. **11**, 892 (2002).
  - [7] C. Castelnovo, R. Moessner and S. L. Sondhi, Nature **451**, 42 (2008).
  - [8] G. Misguich, T. Jolicoeur and S.M. Girvin, Phys. Rev. Lett. **87**, 097203 (2001); T. Jolicoeur, G. Misguich and S.M. Girvin, Progr. Theor. Phys. Suppl. **145**, 76 (2002).
  - [9] D.R. Hofstadter, Phys. Rev. B **14**, 2239 (1976).
  - [10] S. E. Sebastian et al, e-print arXiv:cond-mat/0707.2075 (unpublished).
  - [11] J. Etourneau and P. Hagenmuller, Phil. Mag. B **52**, 589 (1985).
  - [12] PPMS by Quantum Design
  - [13] <http://www.hmi.de/bensc/instrumentation/instrumente/>
  - [14] S. Yoshii et al, J.Phys.: Conf. Ser. **51** 59 (2006).
  - [15] F. Iga et al, J. Magn. Magn. Mater. **310**, e443 (2007).
  - [16] S. Gabáni et al, Acta Phys. Pol. A **113**, 227 (2008).
  - [17] T. Momoi and K. Totsuka, Phys.Rev. B **61**, 3231 (2000).
  - [18] S. Bissola et al, Phys. Rev. B **75**, 184444 (2007).
  - [19] M. Date, J. Phys. Soc. Jpn **57**, 3682 (1988).
  - [20] A. Rauh, G.H. Wannier and G. Obermair, Phys. Status Solidi (b) **63**, 215 (1974)
  - [21] D.J. Thouless et al, Phys. Rev. Lett. **49**, 405 (1982).
  - [22] P. Streda, J. Phys. C:Solid State Phys. **15**, L1299 (1982).
  - [23] D. Springsguth, R. Ketzmerick and T. Geisel, Phys. Rev. B **56**, 2036 (1997).
  - [24] C. Albrecht et al, Physica E **20**, 143 (2003).
  - [25] F. D. M. Haldane and E. H. Rezai, Phys. Rev. Lett. **54**, 237 (1985).